

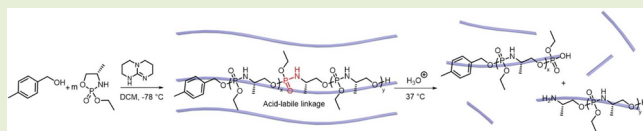
Polyphosphoramidates That Undergo Acid-Triggered Backbone Degradation

Hai Wang, Lu Su, Richen Li, Shiyi Zhang, Jingwei Fan, Fuwu Zhang, Tan P. Nguyen, and Karen L. Wooley*[✉]

Departments of Chemistry, Chemical Engineering, and Materials Science and Engineering, Texas A&M University, College Station, Texas 77842, United States

S Supporting Information

ABSTRACT: The direct and facile synthesis of polyphosphoramidates (PPAs) with acid-labile phosphoramidate backbone linkages are reported, together with demonstration of their hydrolytic degradability, evaluated under acidic conditions. The introduction of acid-labile linkages along the polymer backbone led to rapid degradation of the polymer backbone dependent upon the environmental stimuli. An oxazaphospholidine monomer bearing a phosphoramidate linkage was designed and synthesized to afford the PPAs via organobase-catalyzed ring-opening polymerization in a controlled manner. The hydrolytic degradation of the PPAs was studied, revealing breakdown of the polymer backbone through cleavage of the phosphoramidate linkages under acidic conditions.



Polymeric systems with the ability to degrade under acidic conditions, while being stable under neutral pH, hold great promise for biomedical applications, for instance, the triggered release of therapeutics in cancer and inflammation, among other diseased tissues.^{1–3} The key to such acid-labile polymeric systems is the cleavage of acid-labile bonds, including but not limited to orthoesters,⁴ acetals/ketals,⁵ hydrazones,⁶ and phosphoramidates.⁷ Furthermore, the introduction of acid-labile linkages along the entire polymer backbone could lead to rapid degradation of the polymer backbone, and partial degradation of the backbone linkages could result in a sharp decrease in molecular weights.⁸ The majority of studies on polymers with acid-degradable backbones have focused on acetals/ketals^{9–11} and orthoesters,^{8,12,13} with a few others on hydrazone linkages.^{14,15} However, the labilities of those linkages have limited the choice of polymerization methods, with polycondensation used in most of these reported polymers, resulting in broad molecular weight distributions (\bar{M}) and potentially impeding their applications. Besides polycondensation, polyacetals have also been achieved by acid-catalyzed acetal metathesis (\bar{M} ranging from 1.23 to 2.88, varied by polymer)¹⁶ and cationic ring-opening polymerization (ROP; \bar{M} ranging from 1.3 to 2.0, varied by polymer).¹⁷ Few examples with well-defined polymers containing acid-labile backbone linkages have been reported, including polyacetals achieved by acyclic diene metathesis polymerization,¹⁸ and polyesteracetals achieved by cationic ROP.¹⁹

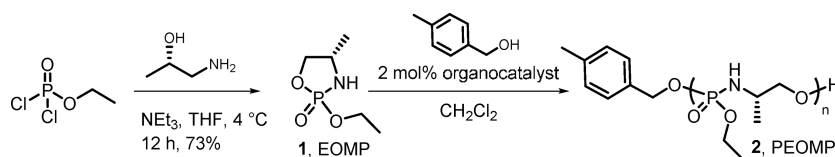
We perceived that the intrinsic basic reaction conditions of organobase-catalyzed ROP made it especially suitable for polymerization of monomers containing acid-labile linkages. In an earlier study, we had demonstrated that phosphoramidate side chain functionalities along the backbone of a polyphosphoester underwent selective side chain cleavage under

acidic conditions.²⁰ Herein, we report the design and synthesis of a unique oxazaphospholidine monomer bearing a phosphoramidate within the cyclic structure to then place that acid-labile linkage along the backbone upon controlled organobase-catalyzed ROP to afford novel well-defined PPAs (Scheme 1).

The monomer, (4S)-2-ethoxy-4-methyl-1,3,2-oxazaphospholidine 2-oxide (EOMP), was synthesized by annulation of ethyl dichlorophosphate with (S)-(+)-2-amino-1-propanol in the presence of trimethylamine (Scheme 1). The annulation reaction was highly efficient, as evidenced by only the EOMP peak being observed in the ³¹P NMR spectrum of the crude product. Purification was then accomplished simply by filtration through a silica gel plug to remove the slight excess amount of triethylamine to give pure EOMP as a highly viscous colorless liquid after concentration. The purity of the monomer was confirmed by mass spectrometry. The ³¹P NMR spectrum of EOMP exhibited resonances at 25.97 and 25.20 ppm (Figure S1c), similar to the ³¹P chemical shift values of reported cyclic phospholane amidate structures.²⁰ The two distinct resonances were attributed to possible geometric isomers arising from the 2-position ethoxy and 4-position methyl groups.²¹ The ¹H NMR and ¹³C NMR spectra (Figure S1a,b) of the monomer also showed two sets of resonances belonging to those two isomers. Resonances in the ¹H NMR spectrum were able to be distinguished through homonuclear correlation spectroscopy (COSY; Figure S2), and the intensities of the resonances revealed the two isomers to be roughly at proportions of 1:1 in the mixture.

Received: December 20, 2016

Accepted: February 15, 2017

Scheme 1. Synthesis and Polymerization of (4*S*)-2-Ethoxy-4-methyl-1,3,2-oxazaphospholidine 2-Oxide (EOMP), 1, to Afford Polymers Bearing Phosphoramidate Linkages along the Backbone, 2


Two organocatalysts, 1,8-diazabicyclo[5.4.0]undec-7-ene (DBU) and 1,5,7-triazabicyclo[4.4.0]dec-5-ene (TBD), which had previously shown excellent control in the ROP of several cyclic phosphorus-containing monomers,^{20,22–25} were used to test the ROP of EOMP (Scheme 1, Table 1). Initially, DBU

Table 1. Polymerization of EOMP Catalyzed by TBD under Different Conditions^a

entry	cat.	<i>T</i> (°C)	[M]/[I]	time (min)	conv. ^b (%)	<i>M</i> _{n, NMR} ^c (kDa)	<i>D</i> ^d
1	TBD	0	100	5	55	9.0	1.10
2	TBD	0	100	10	75	12.2	1.23
3	TBD	0	100	15	88	14.3	1.30
4	TBD	−78	100	60	94	15.2	1.12
5	TBD	−78	50	40	95	7.6	1.08
6	TBD	−78	25	30	94	3.9	1.10

^aThe initiator was 4-methylbenzyl alcohol, the solvent was anhydrous dichloromethane, the monomer concentration was 2.2 M, and catalyst was 2 mol % to monomer for all entries. ^bConversions (conv.) were obtained from ³¹P NMR spectra on aliquots taken from the polymerization mixtures. ^c*M*_{n, NMR} was calculated from the monomer to initiator ratio based on ¹H NMR of final polymer products. ^d*D* was measured by DMF SEC calibrated using polystyrene standards.

was employed as the organocatalyst for the polymerization of EOMP, initiated by 4-methylbenzyl alcohol at room temperature. However, these conditions failed to convert EOMP into its polymer form (PEOMP), even at a relatively high catalyst-to-monomer ratio of 10 mol %. Therefore, DBU was replaced by the stronger catalyst TBD, which has dual activation effects: simultaneously serving as a hydrogen-bond donor to the monomer via the N–H site and also as a hydrogen-bond acceptor to the hydroxyl proton of the propagating alcohol chain end.^{26–28} In the presence of TBD, EOMP polymerization proceeded within 10 min at 0 °C (entries 1–3, Table 1). However, broadening of *D* (1.2–1.3) was observed after the conversion reached greater than 70%, indicating the occurrence of adverse backbiting or transesterification reactions. Therefore, the reaction temperature was decreased to −78 °C (entries 4–6, Table 1). At this reduced temperature, the polymerization remained sufficiently fast to reach over 90% conversion within 1 h, and a narrower *D* (1.08–1.15) was achieved over all conversions from 10 to 94%, indicating the side reactions were successfully avoided.

Unlike most cyclic phospholane ester monomers or reported phosphoramidate^{29–34} monomers,²⁰ EOMP has two distinct directions to open the oxazaphospholidine ring during the polymerization, where either the P–O bond or the P–N bond would be cleaved. Since the p*K*_a of an amine (ca. 38) is significantly larger than that of an alcohol (ca. 16), it was hypothesized that the P–O bond cleavage would be more preferable. A model reaction was carried out at the same condition of the polymerization, while the monomer/initiator feed ratio ([M]₀/[I]₀) was set to be 1. The ³¹P NMR spectrum

of the reaction mixture exhibited resonances at 9.72, 9.57, and 8.54 ppm (Figure S3), which correlated to the phosphoramidate and were consistent with the ³¹P chemical shift values of PEOMP (10.26 ppm; Figure S1f). Furthermore, the ³¹P NMR spectrum showed no resonance at about 12 ppm, corresponding to the phosphoramidate, or about 0 ppm, corresponding to the phosphoester, respectively. These data provided evidence that EOMP had undergone selective cleavage of the P–O bond during the ROP. The kinetics of EOMP ROP were studied using [M]₀/[I]₀ of 100 in dichloromethane with 4-methylbenzyl alcohol as the initiator and TBD as the organocatalyst to monitor the monomer conversions and the growth of polymer chains as a function of time. Monomer conversions were obtained from ³¹P NMR spectra on aliquots taken from the polymerization mixtures. Subsequently, number-average molecular weights (*M*_n) were calculated using ¹H NMR spectra after isolation of the polymer samples by precipitation, with comparison of the intensities of the three 4-methyl protons originating from the initiator on the α-chain end resonating at 2.33 ppm, with the six protons of the two methyl groups on the repeating units resonating at 0.98–1.53 ppm.

The linearity of *M*_n versus monomer conversion (Figure 1a) suggested that the numbers of macromolecules in the reactions remained constant during the polymerizations. The size exclusion chromatography (SEC) traces (Figure 1c) showed unimodal peaks during the reactions, which shifted toward shorter elution times as polymerization progressed while maintaining narrow *D*, below 1.15. Plots of ln([M]₀/[M]) versus time (Figure 1b) showed that the polymerization exhibited first order kinetics, also suggesting the characteristics of a controlled polymerization of the EOMP ROP. Further analysis by matrix-assisted laser desorption/ionization time-of-flight mass spectrometry (MALDI-ToF MS; Figure 1d) of a polymer (DP_n = 10 by ¹H NMR spectroscopy), which had undergone termination by treatment with Amberlyst 15 H-form resin and purification by only one time of precipitation into diethyl ether, revealed two populations, each with a spacing of 165.1 *m/z*, equal to that of the expected monomer repeat unit. Structurally, these two sets of signals were related to the same populations initiated by 4-methylbenzyl alcohol with distinct ionizations. The main peak in the major population at *m/z* = 1811.1 corresponded to a potassium-charged polymer chain of DP_n = 10 that had been initiated by 4-methylbenzyl alcohol and terminated by protonation, further confirming the controlled nature of the polymerization. Meanwhile, the main peak in the minor population at *m/z* = 1912.2 was in agreement with a proton-charged polymer chain of DP_n = 10 having 4-methylbenzyloxy α-end group and proton terminated ω-end group, and 1 equiv of TBD, indicating the strong interaction of TBD with the monomer and the polymer, as well as a possible explanation for the distinct catalytic activity differences between TBD and DBU for the ROP of EOMP. To further investigate

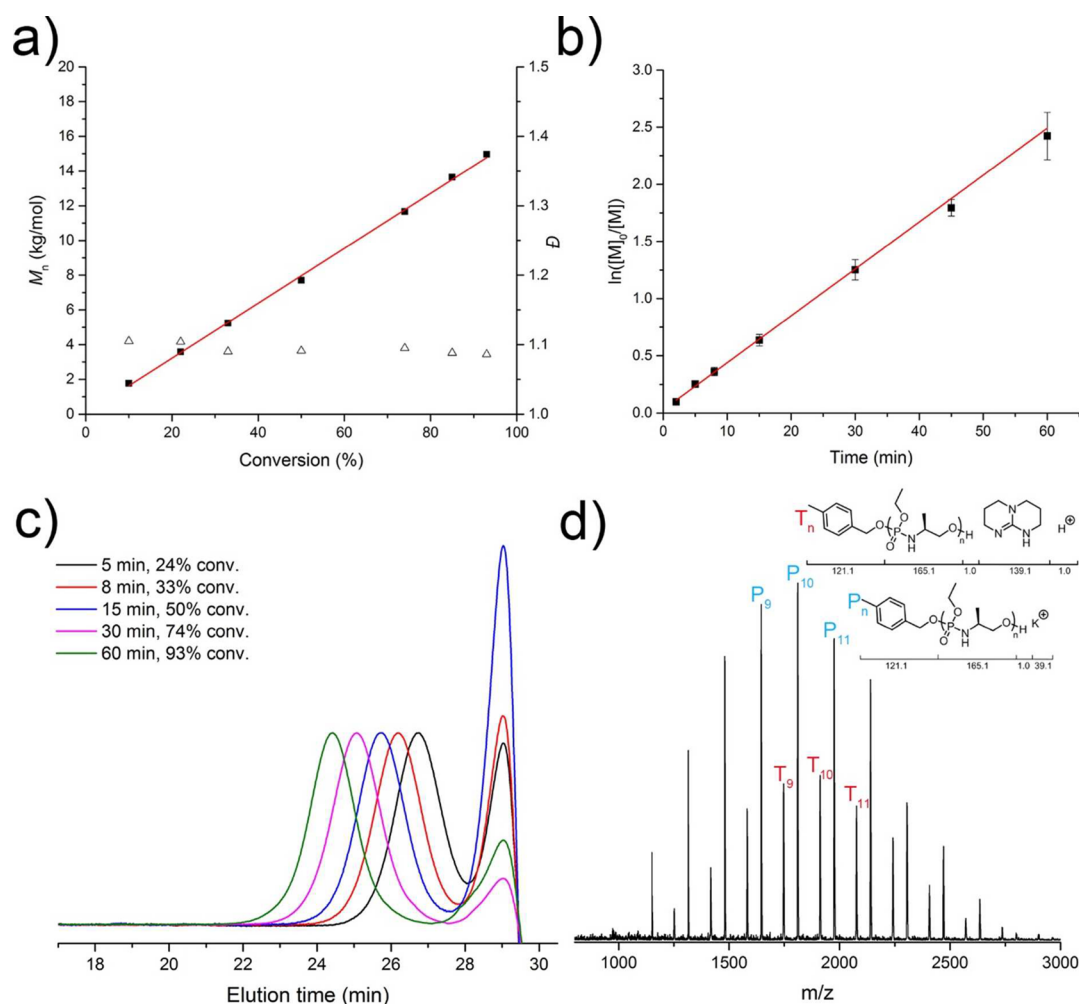


Figure 1. (a) Plot of M_n and D vs monomer conversion for the polymerization of EOMP using TBD as the catalyst and 4-methylbenzyl alcohol as the initiator, obtained from a combination of SEC, ^1H NMR, and ^{31}P NMR spectroscopic analyses. The ratio of monomer/initiator/TBD was 100:1:2. (b) Plots of monomer conversion ($\ln([M]_0/[M])$) vs time obtained from ^{31}P NMR spectra. (c) SEC traces (DMF as eluent, 1 mL/min) of the ROP of EMOP vs time. (d) MALDI-tof MS spectrum of PEMOP ($DP_n = 10$).

the living nature of the polymerization, chain extension of PEOMP was carried out. With addition of EOMP, SEC traces

Figure S4 revealed a shift of the starting PEOMP toward shorter elution time, while maintaining narrow D , below 1.15. By controlling the initial ratio of monomer to initiator, $[M]_0/[I]_0$, as well as the reaction time, a series of PEOMPs with different molecular weights was synthesized. ^{31}P NMR spectra clearly showed only one phosphorus environment at a chemical shift of 10.26 ppm (Figure S1f), and ^1H NMR and ^{13}C NMR spectra (Figure S1d,e) also confirmed the structure of PEOMP. PEOMP appeared as a white to pale yellow powder at room temperature, which was attributed to the glass transition temperature (T_g) of 32–36 °C ($DP_n = 20$ –93). Compared to the reported polyphosphoester PEMEP ($DP_n = 16$ –52, $T_g = -40$ to -37 °C)²² and polyphosphoramidate PMOEPa ($DP_n = 17$ –52, $T_g = -27$ to -19 °C) analogues,²⁰ the T_g of PEOMP was significantly higher, which was attributed to the phosphoramidate linkages along the polymer backbone. PEOMP was highly hygroscopic and would quickly transform from powder to tacky material within minutes and form a viscous solution within hours, if stored open to the air. Furthermore, PEOMP was highly water-soluble, likely attributed to the phosphoramidate backbone linkages and

short pendant ethyl groups, with over 800 mg polymer ($DP_n = 90$) easily dissolved into 1.00 mL of nanopure water within minutes at room temperature.

The phosphoramidate linkages along the polymer backbone also endowed PEOMP with acid-lability. The kinetics of the backbone cleavage of PEOMP ($DP_n = 90$) in aqueous solution was studied in three aqueous buffer solutions with different pH values of 3.0, 5.0, and 7.4. Cleavage of the phosphoramidate linkage, having a ^{31}P resonance at 10.26 ppm, would generate phosphates with distinct ^{31}P chemical shifts at about 0 ppm, allowing for convenient monitoring of the percentage conversion of backbone cleavage by ^{31}P NMR spectroscopy. At pH 7.4 (Figure 2a), the PEOMP was found to be stable for 12.5 d with negligible changes as expected. In the acidic environment, pH 5.0 (Figure 2a), about 27% of the phosphoramidate bonds were cleaved over 12.5 d, and the cleavage reaction reached a plateau at about 8.3 d. At pH 3.0 (Figure 2a), the backbone cleavage was accelerated and about 90% of the phosphoramidate bonds were cleaved within 8–9 d, reaching a plateau at about 9.9 d and about 94% conversion of phosphoramidate-to-phosphate ^{31}P resonance frequencies over 12.5 d. The resonance patterns at each frequency of about 10 and 0 ppm also revealed the progress of backbone cleavage and

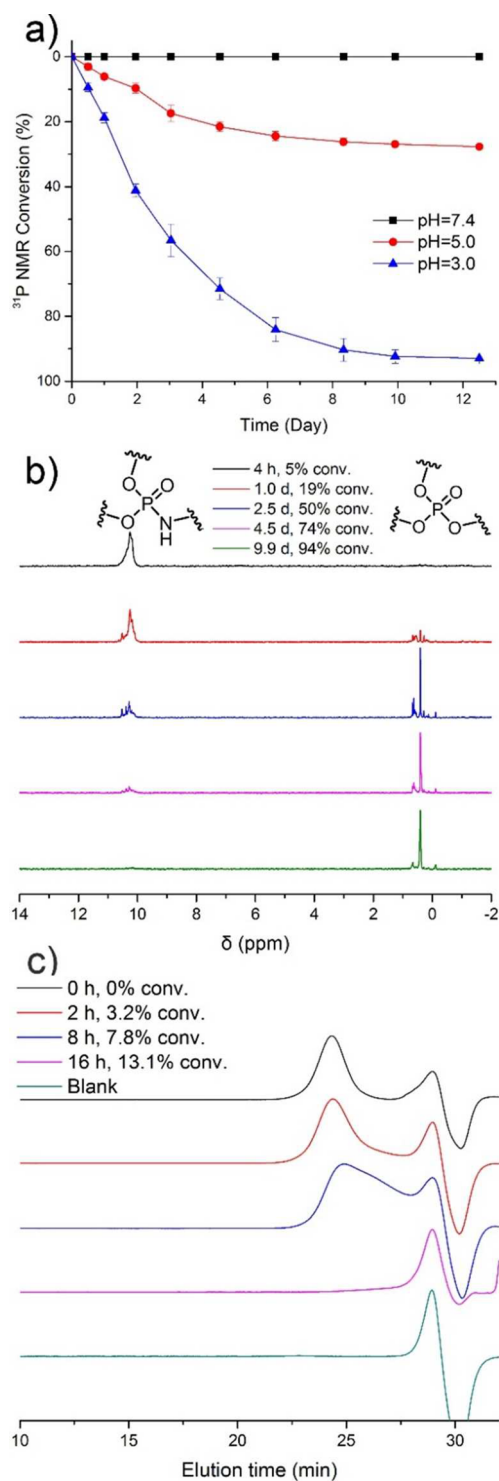


Figure 2. (a) Kinetics of PEOMP degradation at different pH values, as monitored by ³¹P NMR spectroscopy. (b) Transition of ³¹P NMR resonances of PEOMP over a period of conversion at pH 3.0. (c) Progress of the degradation of PEOMP at pH 3.0, as monitored by SEC.

further breakdown of initial phosphates. As shown in Figure 2b, at pH 3.0, over a time range of 4 h to 9.9 d, the conversion increased from 5% to 94% with gradually decreased intensity for the ³¹P resonance at 10.26 ppm, demonstrating the disappearance of the polymer. Over the same time period, sharp resonance signals appeared at 10.53, 10.39, 10.29, and

10.20 ppm with their intensities first increased then decreased, indicating the formation of oligomers and their further degradation into small molecules. The decrease in overall intensity for the combined signals resonating at about 10 ppm was coincident with the appearance of new resonances at 0.67, 0.63, 0.40, 0.29, 0.13, and -0.11 ppm, and their combined growth in intensities over time, suggesting the formation of phosphates. When monitored by SEC, broadening of the peak with increased intensity at longer elution time appeared at 3.2% conversion, while the peak molecular weight (M_p) remained the same, suggesting only a portion of the polymer molecules had been cleaved at this stage. At 7.8% conversion, the M_p shifted to longer elution time with detection of small molecular species, confirming cleavage of a majority of the polymer molecules. At 13.1% conversion, full disappearance of the polymer peak further demonstrated that partial degradation of the backbone linkages resulted in a sharp decrease in molecular weights. Complicating this analysis, however, is the increased affinity to the SEC column for the charged degradation products, relative to the starting PPA.

Therefore, to better understand the molecular weight of the polymer degradation products as a function of % conversion of phosphoramidate backbone linkages, degradation products at different time points were further analyzed by electrospray ionization mass spectrometry (ESI-MS). As shown in Figure S5b, at 40% conversion, ESI-MS revealed one major population with a spacing of 165 m/z equal to that of a monomer, related to the oligomer series E_b (ionized form of 4 in Figure S5a), which resulted directly from the cleavage of phosphoramidate bonds during degradation. The main peak in the major population at $m/z = 512$ corresponding to a trimer was further analyzed by tandem mass spectrometry (MS/MS), and the fragment pattern confirmed the predicted structure (Figure S6). For the whole series of E_b , the major peaks E_1 , E_2 , and E_3 further supported the decrease in molecular weights during backbone degradation, as expected. At 62% conversion (Figure S5c), the signals of series E_b were still dominant, with intensities increased for E_0 and E_1 (relative to E_2) and decreased for higher molecular weight oligomers. In addition, signal intensities of another two populations increased and became more observable, each with a spacing of 165 m/z equal to that of a monomer, corresponding to the oligomer series F_c and G_b . A possible route that could derive series F_c was the hydrolysis of one equivalence of ethyl phosphoester bonds from 5 (Figure S5a), the ω -end counterparts of 4 during the cleavage of the phosphoramidate bond. Unfortunately, signals for the series of 5 were not detected, probably due to their difficulty to be ionized as anions under acidic conditions. Similarly, hydrolysis of one equivalence of ethyl phosphoester bonds from series E_b would result in series G_b (Figure S5a). At 94% conversion (Figure S5d), the signals of series E_b were still dominant, with the major peaks shifted from E_1 to E_0 , while for series F_c and G_b , only F_0 and G_0 were observable, coincident with the high conversion. Furthermore, there was a new series H, observed at 365, 530, 548, 713, and 731 m/z , attributed to ion clusters formed by E_0 with E_1 or E_0 itself (Figures S7 and S8), probably due to the zwitterionic nature of E_0 and E_1 . Series I_a and I_a' , derived from 3 (Figure S5a), the α -end counterparts of 4, were also detected (Figure S9); however, the intensities of the signals were relatively low, while some signals of the I_a and I_a' overlapped with those of H. Since the signal intensities of series E_b were dominant over all conversions, while no notable signal from product of phosphoester bond cleavage besides

series F_c and G_b were observed, the phosphoramidate bonds were demonstrated to be cleaved much faster than the phosphoester bonds under acidic conditions.

Phosphoramidate polymers having the acid-labile phosphoramidate linkage within the backbone are interesting materials that were shown to be prepared readily under basic condition and then undergo selective backbone cleavage reactions under acidic condition. A unique type of stable oxazaphospholidine monomer was synthesized and its organobase-catalyzed ROP kinetics were explored, showing a controlled manner and selective cleavage of P–O bonds during ROP. The resulting highly water-soluble polymers exhibited much higher T_g than their polyphosphoester analogues. Furthermore, the acid-labile phosphoramidate bonds cleaved much faster than the phosphoester bonds under acidic conditions, which enabled the polymer backbone to breakdown rapidly through the cleavage of P–N bonds under acidic conditions. Future studies, including synthesis of acid-labile nanostructured materials, as well as controlling the acidolysis rate of the polymer, are being actively pursued.

■ ASSOCIATED CONTENT

● Supporting Information

The Supporting Information is available free of charge on the ACS Publications website at DOI: [10.1021/acsmacrolett.6b00966](https://doi.org/10.1021/acsmacrolett.6b00966).

Detailed experimental section, images, and tables (PDF).

■ AUTHOR INFORMATION

Corresponding Author

*E-mail: wooley@chem.tamu.edu. Tel.: (979) 845-4077.

ORCID

Karen L. Wooley: [0000-0003-4086-384X](https://orcid.org/0000-0003-4086-384X)

Notes

The authors declare no competing financial interest.

■ ACKNOWLEDGMENTS

We gratefully acknowledge financial support from the National Science Foundation under Grant Nos. DMR-1507429 and DMR-1309724. The Welch Foundation is gratefully acknowledged for support through the W. T. Doherty-Welch Chair in Chemistry, Grant No. A-0001. Use of the TAMU/LBMS is acknowledged.

■ REFERENCES

- (1) Binauld, S.; Stenzel, M. H. *Chem. Commun.* **2013**, 49 (21), 2082–2102.
- (2) Meng, F.; Zhong, Y.; Cheng, R.; Deng, C.; Zhong, Z. *Nanomedicine* **2014**, 9 (3), 487–499.
- (3) Pang, X.; Jiang, Y.; Xiao, Q.; Leung, A. W.; Hua, H.; Xu, C. J. *Controlled Release* **2016**, 222, 116–129.
- (4) Tang, R.; Ji, W.; Panus, D.; Palumbo, R. N.; Wang, C. J. *Controlled Release* **2011**, 151 (1), 18–27.
- (5) Zhang, Q.; Hou, Z.; Louage, B.; Zhou, D.; Vanparijs, N.; De Geest, B. G.; Hoogenboom, R. *Angew. Chem., Int. Ed.* **2015**, 54 (37), 10879–10883.
- (6) Cui, J.; Yan, Y.; Wang, Y.; Caruso, F. *Adv. Funct. Mater.* **2012**, 22 (22), 4718–4723.
- (7) Zhang, L.; Jeong, Y.-I.; Zheng, S.; Jang, S. I.; Suh, H.; Kang, D. H.; Kim, I. *Polym. Chem.* **2013**, 4 (4), 1084–1094.
- (8) Li, L.; Xu, Y.; Milligan, I.; Fu, L.; Franckowiak, E. A.; Du, W. *Angew. Chem., Int. Ed.* **2013**, 52 (51), 13699–13702.
- (9) Jain, R.; Standley, S. M.; Fréchet, J. M. J. *Macromolecules* **2007**, 40 (3), 452–457.
- (10) Liu, N.; Vignolle, J.; Vincent, J.-M.; Robert, F.; Landais, Y.; Cramail, H.; Taton, D. *Macromolecules* **2014**, 47 (5), 1532–1542.
- (11) Paramonov, S. E.; Bachelder, E. M.; Beaudette, T. T.; Standley, S. M.; Lee, C. C.; Dashe, J.; Fréchet, J. M. J. *Bioconjugate Chem.* **2008**, 19 (4), 911–919.
- (12) Wang, C.; Ge, Q.; Ting, D.; Nguyen, D.; Shen, H.-R.; Chen, J.; Eisen, H. N.; Heller, J.; Langer, R.; Putnam, D. *Nat. Mater.* **2004**, 3 (3), 190–196.
- (13) Schacht, E.; Toncheva, V.; Vandertaelen, K.; Heller, J. J. *Controlled Release* **2006**, 116 (2), 219–225.
- (14) Jeong, M. J.; Kim, B. J.; Chang, J. Y. *J. Polym. Sci., Part A: Polym. Chem.* **2002**, 40 (24), 4493–4497.
- (15) Zhou, L.; Yu, L.; Ding, M.; Li, J.; Tan, H.; Wang, Z.; Fu, Q. *Macromolecules* **2011**, 44 (4), 857–864.
- (16) Pemba, A. G.; Flores, J. A.; Miller, S. A. *Green Chem.* **2013**, 15 (2), 325–329.
- (17) Whiting, B. T.; Coates, G. W. *J. Am. Chem. Soc.* **2013**, 135 (30), 10974–10977.
- (18) Khaja, S. D.; Lee, S.; Murthy, N. *Biomacromolecules* **2007**, 8 (5), 1391–1395.
- (19) Neitzel, A. E.; Petersen, M. A.; Kokkoli, E.; Hillmyer, M. A. *ACS Macro Lett.* **2014**, 3 (11), 1156–1160.
- (20) Zhang, S.; Wang, H.; Shen, Y.; Zhang, F.; Seetho, K.; Zou, J.; Taylor, J.-S. A.; Dove, A. P.; Wooley, K. L. *Macromolecules* **2013**, 46 (13), 5141–5149.
- (21) Penczek, S.; Pretula, J.; Kaluzynski, K. *Biomacromolecules* **2005**, 6 (2), 547–551.
- (22) Steinbach, T.; Schroder, R.; Ritz, S.; Wurm, F. R. *Polym. Chem.* **2013**, 4 (16), 4469–4479.
- (23) Zhang, S.; Li, A.; Zou, J.; Lin, L. Y.; Wooley, K. L. *ACS Macro Lett.* **2012**, 1 (2), 328–333.
- (24) Steinbach, T.; Ritz, S.; Wurm, F. R. *ACS Macro Lett.* **2014**, 3 (3), 244–248.
- (25) Zhang, S.; Zou, J.; Zhang, F.; Elsabahy, M.; Felder, S. E.; Zhu, J.; Pochan, D. J.; Wooley, K. L. *J. Am. Chem. Soc.* **2012**, 134 (44), 18467–18474.
- (26) Dove, A. P. *ACS Macro Lett.* **2012**, 1 (12), 1409–1412.
- (27) Clément, B.; Grignard, B.; Koole, L.; Jérôme, C.; Lecomte, P. *Macromolecules* **2012**, 45 (11), 4476–4486.
- (28) Iwasaki, Y.; Yamaguchi, E. *Macromolecules* **2010**, 43 (6), 2664–2666.
- (29) Yilmaz, Z. E.; Jérôme, C. *Macromol. Biosci.* **2016**, 16 (12), 1745–1761.
- (30) Sun, C.-Y.; Dou, S.; Du, J.-Z.; Yang, X.-Z.; Li, Y.-P.; Wang, J. *Adv. Healthcare Mater.* **2014**, 3 (2), 261–272.
- (31) Zhai, X.; Huang, W.; Liu, J.; Pang, Y.; Zhu, X.; Zhou, Y.; Yan, D. *Macromol. Biosci.* **2011**, 11 (11), 1603–1610.
- (32) Liu, J.; Pang, Y.; Huang, W.; Zhai, X.; Zhu, X.; Zhou, Y.; Yan, D. *Macromolecules* **2010**, 43 (20), 8416–8423.
- (33) Zhang, F.; Smolen, J. A.; Zhang, S.; Li, R.; Shah, P. N.; Cho, S.; Wang, H.; Raymond, J. E.; Cannon, C. L.; Wooley, K. L. *Nanoscale* **2015**, 7 (6), 2265–2270.
- (34) Sun, R.; Du, X.-J.; Sun, C.-Y.; Shen, S.; Liu, Y.; Yang, X.-Z.; Bao, Y.; Zhu, Y.-H.; Wang, J. *Biomater. Sci.* **2015**, 3 (7), 1105–1113.